

Correlated Spectral And Temporal Behaviour Of Late-Time Afterglows Of Gamma Ray Bursts

Shlomo Dado¹ and Arnon Dar¹

ABSTRACT

The cannonball (CB) model of gamma ray bursts (GRBs) predicts that the asymptotic behaviour of the spectral energy density of the X-ray afterglow of GRBs is a power-law in time and in frequency where the difference between the temporal and spectral power-law indexes, $\alpha_X - \beta_X$, is restricted to the values 0, 1/2 and 1. Here we report the distributions of the values α_X , β_X and their difference for a sample of 315 Swift GRBs. This sample includes all Swift GRBs that were detected before August 1, 2012, whose X-ray afterglow extended well beyond 1 day and the estimated error in $\alpha_X - \beta_X$ was ≤ 0.25 . The values of α_X were extracted from the CB model fits to the entire light curves of their X-ray afterglow while the spectral index was extracted by the Swift team from the time integrated X-ray afterglow of these GRBs. We found that the distribution of the difference $\alpha_X - \beta_X$ for these 315 Swift GRBs has three narrow peaks around 0, 1/2 and 1 whose widths are consistent with being due to the measurement errors, in agreement with the CB model prediction.

Subject headings: gamma rays: bursts

1. Introduction

A major breakthrough in the study of gamma ray bursts (GRBs) was the discovery of their X-ray afterglow by the Beppo-SAX satellite (Costa, E. et al. 1997), which led to their localization and consequently to the discovery of their longer wave-length afterglows (van Paradijs et al. 1997, Frail & Kulkarni 1997), which were predicted (Paczynski & Roads 1993, Katz 1994, Mezaros & Rees 1997) by the fireball model of GRBs (Paczynski 1986, Goodman 1986). Until the launch of the Swift satellite, the fireball model was widely accepted as the correct model of GRBs and their afterglows (see, e.g., the reviews by Meszaros 2002, Zhang & Meszaros 2004, Piran 2004). The rich data on GRBs and their afterglows obtained in recent

¹Physics Department, Technion, Haifa 32000, Israel

years with the Swift and Fermi satellites complemented by data from ground-based rapid response telescopes and large follow-up telescopes, however, have challenged this prevailing view (see, e.g., Dar 2006 and the publications of Dado et al. cited in this paper and references therein; Margutti et al. 2012 and references therein).

In contrast, the cannonball model (CB) of GRBs (Dar & De Rújula 2004 and references therein) has been very successful in reproducing also the detailed light-curves of GRBs and their AGs that were measured with the Swift and Fermi satellites (see, e.g., Dado et al. 2009a,b). This success required adjustment of the free parameters of the CB model to fit the data, which could have made one wonder whether the good agreement between theory and observations was due to the flexibility of the model rather than to its validity.

The CB model, however, has been used also to predict universal properties of GRBs and their afterglows *before their discovery by observations*, which do not depend on free or adjustable parameters. For the prompt emission, these included the large linear polarization of the prompt gamma rays¹ (e.g., Shaviv & Dar 1995), the rapid spectral softening that accompanied the fast decline of the prompt γ -ray emission (see, e.g., Dado et al. 2007 and references therein), and several correlations among GRB observables (see, e.g., Dar & De Rújula 2000, Dado & Dar 2012 and references therein) including the ‘Amati relation’ (Amati et al. 2002).

As for the afterglow emission, the CB model predicted the appearance of an underlying supernova in the optical AG of relatively nearby long duration GRBs (see, e.g., Dar 1999, Dado et al. 2002, 2003 and references therein), the canonical behaviour of X-ray light-curves - the transition to a plateau phase after a fast decline with a rapid softening of the prompt emission spectral energy density (SED) that bends/breaks smoothly into an asymptotic power-law decline (e.g., Dado et al. 2002, Dar & De Rújula 2004) - before it was discovered with Swift (Nousek et al. 2006), and the chromatic behaviour of the broad-band (XUVONIR) afterglow at early time (e.g., Covino et al. 2006) that becomes achromatic well after the smooth bend/break time with roughly a universal spectral index $\beta_{U\!V\!O\!N\!I\!R} \approx \beta_X \approx 1.1^2$.

In this paper, we have used the CB model to derive another universal feature of the late-time broad band (XUVONIR) afterglow of GRBs, which does not involve adjustable parameters. Namely, we show that in the CB model the observed pectral energy density of the *late-time* afterglow declines with time and frequency, like $F_\nu(t) \sim t^{-\alpha_\nu} \nu^{-\beta_\nu}$ where the

¹Such evidence was reported by Coburn & Boggs 2003 (see, however, Rutledge & Fox 2004 and Wigger et al. 2004), Willis et al. 2005, McGlynn et al. 2007, Gotz et al. 2009 and Yonetoku et al. 2011.

²This behaviour was predicted only for late-time non-flaring afterglows.

difference between the temporal and spectral power-law indexes can have one of the values $\alpha_\nu - \beta_\nu = 0, 1/2$ or 1 . This closure relation then was tested using the 0.3-10 keV light-curves of the X-ray afterglow of 315 Swift GRBs, which were measured accurately enough well beyond 1 day with the Swift X-ray telescope (XRT). The CB model best fits to the entire available data of their X-ray afterglows were used to extract the values of their late-time temporal index α_X , while the values of their spectral index β_X were those inferred by the Swift team from the spectrum of the time integrated X-ray afterglow.

2. The synchrotron radiation afterglow at late time

In the CB model (see, e.g., Dar & De Rújula 2004, Dado et al. 2002, 2009a and references therein) GRBs and their afterglows are produced by the interaction of bipolar jets of highly relativistic plasmoids (CBs) of ordinary matter with the radiation and matter along their trajectory (Shaviv & Dar 1995, Dar 1998). Such jetted CBs are presumably ejected in accretion episodes on the newly formed compact stellar object in core-collapse supernova (SN) explosions (Dar et al. 1992, Dar & Plaga 1999, Dar & De Rújula 2000), in the merger of compact objects in close binary systems (Goodman et al. 1987, Shaviv & Dar 1995) and in mass accretion episodes in microquasars and phase transitions in compact stars (Dar 1998, Dado et al. 2009b).

In the CB model, the circumburst medium in front of a highly relativistic CB is completely ionized by the radiation from the CB. In the CB's rest frame, the ions of the medium that are continuously impinging on the CB generate within it a turbulent magnetic field, whose energy density is assumed to be in approximate equipartition with that of the impinging particles, $B \approx \sqrt{4\pi n m_p c^2} \gamma$ (e.g., Dado et al. 2002), where n is the external baryon density and m_p is the proton mass. The electrons that enter the CB with a relative Lorentz factor $\gamma'_e(t) = \gamma(t)$ in the CB's rest frame are Fermi accelerated there to a smoothly broken power-law distribution in γ'_e with a break around $\gamma'_e(t) = \gamma(t)$ and a power-law index $p_e \sim 2.1$ well above it. These electrons cool rapidly by emission of synchrotron radiation (SR). This SR is isotropic in the CB's rest frame and has a smoothly broken power-law with a characteristic break frequency $\nu'_b(t)$, which is the typical synchrotron frequency radiated by the interstellar medium (ISM) electrons that enter the CB at time t with a Lorentz factor $\gamma(t)$. In the observer frame, the emitted photons are beamed into a narrow cone along the CB's direction of motion by its highly relativistic bulk motion, their arrival times are aberrated and their energies are boosted by its bulk motion Doppler factor δ and redshifted by the cosmic expansion during their travel time to the observer. In particular, in the observer

frame (see, e.g. Eq. (25) in Dado et al. 2009a),

$$\nu_b(t) = \delta(t) \nu'_b(t)/(1+z) \propto n^{1/2} [\gamma(t)]^3 \delta(t), \quad (1)$$

where $\delta = 1/\gamma(1 - \beta \cos\theta)$ is its Doppler factor with θ being the angle between the line of sight to the CB and its direction of motion. For $\gamma^2 \gg 1$ and $\theta^2 \ll 1$, $\delta \approx 2\gamma/(1 + \gamma^2\theta^2)$ to an excellent approximation. The spectral energy density of the *unabsorbed* SR afterglow has the form (see, e.g., Eq. (26) in Dado et al. 2009a),

$$F_\nu \propto n^{(\beta_\nu+1)/2} [\gamma(t)]^{3\beta_\nu-1} [\delta(t)]^{\beta_\nu+3} \nu^{-\beta_\nu}, \quad (2)$$

where the spectral index β_ν of the emitted radiation is related to the power-law index p_e of the Fermi accelerated electrons through $\beta_\nu = p_e/2$ for $\nu > \nu_b$ and $\beta_\nu = (p_e - 1)/2$ for $\nu < \nu_b$. The photon spectral index of the unabsorbed X-ray afterglow and the photon spectral index of the emitted radiation is given by $\Gamma_\nu = \beta_\nu + 1$.

The intercepted ISM particles that are swept into the CB decelerates its motion. For a CB of a baryon number N_B , a radius R and an initial Lorentz factor $\gamma_0 \gg 1$, which propagates in an ISM of a constant density n , relativistic energy-momentum conservation for plastic collisions yields the deceleration law (Dado et al. 2009b and references therein):

$$\gamma(t) = \frac{\gamma_0}{[\sqrt{(1 + \theta^2 \gamma_0^2)^2 + t/t_0} - \theta^2 \gamma_0^2]^{1/2}}, \quad (3)$$

where $\gamma_0 = \gamma(0)$ and $t_0 = (1+z) N_B/8cn\pi R^2 \gamma_0^3$.

As can be seen from Eqs. (2) and (3), for a constant-density ISM, the shape of the light-curve of the AG depends on only three parameters: the product $\gamma_0 \theta$, the deceleration time scale t_0 and the spectral index $\beta(t)$. As long as $t \lesssim t_b = (1 + \theta^2 \gamma_0^2)^2 t_0$, $\gamma(t)$ and consequently $\delta(t)$, $\nu_b(t)$ and $\beta(t)$ change rather slowly with t and generate the plateau phase of $F_\nu(t)$. For $t \gg t_b$, Eq. (3) yields $\gamma(t) \propto t^{-1/4}$. Thus, for late time ($t \gg t_b$), $[\gamma(t)\theta]^2$ becomes $\ll 1$, $\delta \approx 2\gamma(t)$ and ν_b decreases to well below the UVONIR bands ($\beta \approx \beta_X \approx 1.1$). Consequently, Eq. (2), yields a universal achromatic power-law behaviour of the late-time ($t \gg t_b$) broadband XUVONIR AG,

$$F_\nu(t) \propto [\gamma(t)]^{(4\beta_X+2)} \nu^{-\beta_X} \propto t^{-(\beta_X+1/2)} \nu^{-\beta_X}, \quad (4)$$

where $\alpha - \beta = \alpha_X - \beta_X = 1/2$. Such a canonical behaviour of the X-ray afterglow of GRBs is demonstrated in Figure 1 where the 0.3-10 keV X-ray light-curve of GRB 060729 that was measured with the Swift XRT is plotted together with its CB model best fit light-curve.

Often the break of the X-ray afterglow of very luminous GRBs is hidden under the prompt GRB emission or its fast decline phase (this happens because γ_0 is rather large and

$[\gamma_0 \theta]^2 \ll 1$ yielding a rather small t_b). In such GRBs the "late-time" power-law decline of the X-ray AG begins right after the fast decline of the prompt emission with the canonical late-time temporal index $\alpha_X = \beta_X + 1/2$ (Dado et al. 2008). This is demonstrated in Figure 2 where the light-curve of the X-ray afterglow of GRB 061007 that was measured with the Swift XRT is plotted together with its CB-model best fit light-curve.

Consider now a CB that encounters a wind-like density profile $n \sim n_0 (r_0/r)^2$ at $r = r_0$. For simplicity, let us set the encounter time to be $t = 0$ in the observer frame. As long as the CB has not yet swept in a relativistic mass comparable to its mass, γ and δ change rather slowly as a function of time and stay put at their values at $t = 0$. Hence, $r - r_0 \approx \gamma(0) \delta(0) ct/(1+z) \propto t$. Consequently, as long as the CB has not swept in a relativistic mass comparable to its rest mass, Eqs. (2) and (1) yield for a wind-like density profile

$$F_\nu \propto n^{(1+\beta_X)/2} \nu^{-\beta_X} \propto t^{-(1+\beta_X)} \nu^{-\beta_X}. \quad (5)$$

Consequently, $\alpha_X = \Gamma_X$, i.e., $\alpha_X - \beta_X = 1$. (Dado et al. 2009a). A GRB produced near the center of an elliptical galaxy may have an X-ray afterglow with such a late-time behaviour. This is demonstrated in Figure 4 where we plotted the light-curve of the X-ray afterglow of the short GRB 060414 and its CB model best fit light-curve.

In the CB model, the prompt emission pulses are produced by different CBs which, for simplicity, are assumed to be emitted in the same direction. The time resolution during the afterglow phase is usually much longer than the time separation between the prompt GRB pulses, i.e., the separation between the CBs' emission times, which, coupled with the initial fast expansion of the CBs and their merger due to the deceleration of the leading one in the ISM, allow us to consider them as a single blob during the afterglow phase (see e.g. Dar & De Rújula 2004), which we have so far done.

However, if the ejecta has a "shot gun" distribution, i.e., consist of many ($N_{CB} \gg 1$) CBs, which are spread within a small angle θ_e ($1/\gamma(0) \ll \theta_e \ll 1$), then one must integrate their contribution taking into account their different viewing angles. In the limit of a uniform angular distribution of CBs within an angle θ_e (namely, an angular density $N_{CB}/\pi \theta_e^2$) and neglecting the spread in arrival times from different CBs at late time, the simple integration of Eq. (1) over θ for an on-axis observer yields the *late-time* SED,

$$F_\nu(t) \propto [\gamma(t)]^{4\beta_X} \nu^{-\beta_X} \propto t^{-\beta_X} \nu^{-\beta_X} \quad (6)$$

i.e., $\alpha_X = \beta_X$ and hence, $\alpha - \beta = \alpha_X - \beta_X = 0$ and $\nu_b(t) \sim t^{-\alpha_X/\beta_X} \rightarrow t^{-1}$ at late time. These results are valid also for observers slightly off-axis because the integration over viewing angle is dominated by the contribution from CBs moving near the line of sight. In Figure 5 we have plotted the 0.3-10 keV X-ray afterglow of GRB 110808A that was retrieved from

the Swift/XRT light-curve repository (Evans et al. 2007, 2009) and its CB-model best fit light-curve assuming a shot-gun configuration of CBs.

All together, the CB model predicts that the late-time temporal decay of the GRB afterglow is well approximated by power-law with a power-law index α_ν that is simply related to the spectral index β_ν of the late-time afterglow. In particular it predicts that error-free measurements of the late-time $\alpha_X - \beta_X$, must yield a triple-peak distribution with narrow peaks around 0, 1/2 and 1 provided that the circumburst environments are well represented by the assumed constant density ISM or a wind-like density profile.

Note, however, that while the CB model predicts a triple peak distribution of $\alpha - \beta$ at late time, it predicts a single-peak distribution of the late-time β around 1.083 and a late-time power-law decay of ν_b with a temporal index that is peaked around -1.083 (e.g., Dar and De Rújula 2004, 2007).

3. Comparison with observations

Reliable and accurate values of the temporal and spectral power-law indexes α_X and β_X of the late-time X-ray afterglow measured with the Swift XRT, which are reported in the Swift/XRT light-curve repository (Evans et al. 2007, 2009), often are difficult to obtain because of one or more of the following reasons:

- (a) The XRT measurements often run out of statistics or approach the background level before α_X reaches its late-time constant value.
- (b) Temporal gaps in the late-time data.
- (c) Flares that are superimposed on the presumably smooth afterglow light-curves.
- (d) A too simplistic model of extragalactic absorption restricted to the host galaxy whose chemical composition is taken to be solar and independent of redshift, that is used to infer Γ_X . Moreover, GRBs without known redshift are treated as GRBs at redshift $z = 0$.

Before the launch of the Swift satellite, the knowledge of the X-ray afterglow of GRBs was incomplete and its inferred behaviour from limited and patchy data appeared to agree with the fireball model predictions (Meszaros and Rees 1997; Sari et al. 1998). After the launch of the Swift satellite it became rather clear that the observed properties and the diversity of the measured X-ray-afterglows, both at early and late times, challenge the fireball model paradigm (see, e.g., Dar 2006 and the other publications of Dado et al. cited in the bibliography, and the references therein). This led to empirical parametrizations of AG light-curves such as smoothly broken power-laws (e.g., Beuermann et al. 1999) exponential to power-law functions (e.g., Willingale et al. 2007), and smoothly broken segmented

power-laws (e.g., Margutti et al. 2012), which have never been derived from an underlying physical model. In most cases it was possible to fit reasonably well the observational data by introducing sufficient number of free adjustable parameters. However, because of difficulties (a)-(d) and the scarcity of late-time data it was not clear whether the extrapolation of these fits to late times yields reliable values of the late-time (asymptotic) α_X .

In contrast, the CB model light-curves summarized in Eqs. (1)-(2), which were derived in fair approximations from the underlying assumptions of the CB model, were shown to describe very well the observed X-ray light-curves of the X-ray AGs of a large sample (over 150) of Swift GRBs with known redshift, including those with superimposed early-time and late-time flares (see, e.g., Dado et al. 2009a,b; Dado and Dar 2010 and references therein). In particular, their underlying smooth component was fitted very well by Eqs. (1)-(2) only with three adjustable parameters, $\gamma_0 \theta$, t_b and $p_e = 2\beta_X$ and the properly chosen circumburst environment (a constant density or a wind-like density profile). This is demonstrated in Figures 1-6.

Thus, in order to avoid difficulties (a)-(d) and empirical parametrizations of the X-ray AG, we have extracted the late-time temporal slope α_X from the asymptotic power-law behaviour as given by Eqs. (4)-(6) of the cannonball model fits to the entire X-ray light-curve. Moreover, since the late-time behaviour of the X-ray AG is independent of redshift, we have extended our fits to all the 315 X-ray light-curves that were reported in the Swift/XRT light-curve repository (Evans et al. 2007, 2009) before August 1, 2012, with or without known redshift, whose measured 0.3-10 keV X-ray AG extended beyond 1 day and the reported error in their inferred spectral index is ≤ 0.25 . The typical error in the values of α_X obtained from the CB model fits to the entire 0.3-10 keV light-curve of the X-ray AG of the Swift GRBs was much smaller than the typical error in the inferred value of Γ_X that was reported in the Swift/XRT light-curve repository (Evans et al. 2007,2009).

We caution that the values of the late-time α_X that were obtained from the CB model best fit light-curves of the entire X-ray afterglow may differ significantly from those obtained from empirical parametrizations of the light-curves and arbitrary selection of time intervals. For instance, the CB model best fit light-curve of the smooth 0.3-10 keV light-curve of the X-ray afterglow of GRB 090618 that is shown in Figure 6, yielded $\gamma_0 \theta = 0.707$, $t_b = 2953$ s and $p_e = 2.084$ i.e., a late-time $\alpha_X = 1.584 \pm 0.03$ ($\chi^2/dof = 1.06$ for $dof=1301$) while a smoothly broken power-law (Beuermann et al. 1999) fit yields $\alpha_1 = 0.79 \pm 0.01$, a break time $t_b = 0.50 \pm 0.11$ d and a late-time $\alpha_X = \alpha_2 = 1.74 \pm 0.04$ ($\chi^2/dof = 1.17$). The best fit spectral index of the unabsorbed 0.3-10 keV spectrum of the afterglow ($t > 250$ s) is $\beta_X = 1.04 \pm 0.04$. The CB model prediction $\alpha_X = \beta_X + 1/2 = 1.54 \pm 0.04$ is consistent with the value $\alpha_X = 1.584$ inferred from the CB model best fit light-curve of the 0.3-10 keV

X-ray AG of GRB 090618 reported in the Swift/XRT light-curve repository (Evans et al. 2007, 2009), but is inconsistent with the value inferred from the smoothly broken power-law parametrization of the AG.

In Figure 7 we have plotted the values of Γ_X of the time-integrated 0.3-10 keV X-ray AG of the 315 Swift GRBs, which were retrieved from the Swift/XRT light-curve repository. Their distribution is shown in Figure 8. As can be seen from Figures 7 and 8, their distribution peaks around the canonical value $\Gamma_X = 25/12$ of the cannonball model, which is represented by the horizontal and vertical lines, respectively, in Figures 7 and 8.

In Figure 9 we have plotted the values of late-time slope α_X of the X-ray AG of the 315 GRBs plotted in Figures 7 and 8 that were obtained from the CB model best fit light-curves of the 0.3-10 keV X-ray AGs observed with the Swift XRT. These slopes seem to cluster around the canonical values 2.1, 1.6 and 1 of the CB model as is indicated by their distribution, which is plotted in Figure 10. This clustering is much more evident in Figures 11 and 12 where the values of $\alpha_X - \beta_X$ and their distribution are shown for the 315 GRBs plotted in Figure 7. The horizontal and vertical lines in Figures 11 and 12, respectively, represent the CB model expectation $\alpha_X - \beta_X = 0, 1/2, \text{ or } 1$ for error-free measurements.

4. Conclusion

: The spectral energy density of the X-ray afterglow of 315 ordinary GRBs detected before August 1, 2012, which have a late-time X-ray AG that was well measured with the Swift/XRT, is well described by a simple power-law in time and frequency, $F_\nu(t) \sim t^{-\alpha} \nu^{-\beta}$. Their X-ray afterglows are well described by the CB model (e.g., Dado et al. 2009a). The distribution of the difference between the late-time temporal and spectral power-law indexes $\alpha_X - \beta_X$ extracted from their CB model fits has a triple peak structure with peaks around 0, 1/2 and 1 of full widths at half maximum consistent with the measurement errors while the distribution of β_X has only a single peak around 1.08. This behaviour is in good agreement with the CB-model prediction that the difference between the late-time temporal and spectral power-law indexes of GRBs is restricted to the values 0, 1/2 or 1, while such a behaviour challenges alternative GRB models.

Acknowledgement: The authors would like to thank an anonymous referee for useful comments and suggestions.

REFERENCES

- Amati, L., et al. 2002, *A&A* 390, 81
- Beuermann, K., et al. 1999, *A&A*, 352, L26
- Cano, Z., et al. 2011, *MNRAS*, 413, 669
- Coburn, W. & Boggs, S. E. 2003, *Nature*, 423, 415
- Costa, E., et al 1997, *Nature*, 387, 783
- Covino, S., et al. 2006, *Nuovo Cimento*, 121B, 1171
- Dado, S., & Dar, A. 2012, arXiv:1203.5886
- Dado, S., Dar, A. & De Rújula, A. 2002, *A&A*, 388, 1079
- Dado, S., Dar, A. & De Rújula, A. 2003, *ApJ*, 594, L89 (arXiv:astro-ph/0304106)
- Dado, S., Dar, A. & De Rújula, A. 2007, *ApJ*, 663, 400
- Dado, S., Dar, A. & De Rujula, A. 2008, *ApJ*, 680, 517
- Dado, S., Dar, A. & De Rújula, A. 2009a, *ApJ*, 696, 994
- Dado, S., Dar, A. & De Rújula, A. 2009b, *ApJ*, 693, 311
- Dar, A. 1998, *ApJ*, 500, L93
- Dar, A. 1999, *GCN Report* 346
- Dar, A., 2006, *Chin. J. Astron. Astrophys.* 6, 323, 206 (arXiv:astro-ph/0511622)
- Dar, A., & De Rújula, A. 2000, arXiv:astro-ph/0008474
- Dar, A. & De Rújula, A. 2004, *Phys. Rep.* 405, 203
- Dar, A. & De Rújula, A. 2008, *Phys. Rep.* 466, 179
- Dar, A., et al. 1992, *ApJ*, 388, 164
- Dar, A. & Plaga, R. 1999, *A&A*, 349, 259
- Evans P.A., et al., 2007, *A&A*, 469, 379
- Evans, P.A. et al. 2009, *MNRAS*, 397, 1177

- Frail, D. A., & Kulkarni, S. R. 1997, IAU Circ. No. 6662
- Goodman, J., 1986 ApJ, 308, L47
- Goodman, J., Dar, A. & Nussinov, S. 1987, ApJ, 314, L7
- Gotz, D., et al., 2009, ApJ, 695, L208
- Katz, J., 1994, ApJ, 432, L107
- Margutti, R., et al. 2012, arXiv:1203.1059
- McGlynn, S., et al. 2007, A&A, 466, 895
- Meszáros, P. 2002, Ann. Rev. ARAA, 40, 137
- Meszáros, P. & Rees, M. J. 1997, ApJ, 476, 232
- Nousek, J. A., et al. 2006, ApJ, 642, 389
- Paczynski, B. 1986, ApJ, 308, L43
- Paczynski, B. & Rhoads, J. E. (1993), ApJ, 418, L5
- Piran, T. 2004, Reviews of Modern Physics, 76, 1143
- Rutledge, R. E. & Fox, D. B. 2004, MNRAS, 350, 1272
- Sari R., Piran T. & Narayan R. 1998, ApJ, 497, L17
- Shaviv, N. J. & Dar, A. 1995, ApJ, 447, 863
- van Paradijs, J. et al. 1997, Nature 386, 686
- Wigger, C., et al. 2004, ApJ, 613, 1088
- Willingale R., et al. 2007, ApJ, 662, 1093
- Willis, D. R., et al. 2005, A&A, 439, 245
- Yonetoku, D., et al. 2011, ApJ, 743, L30
- Zhang, B., & Meszaros, P. 2004, Int. J. Mod. Phys. A, 19, 2385

Table 1. The best fit parameters of the CB model description of the light-curves of the 0.3-10 keV X-ray afterglow of a representative sample of GRBs measured with Swift/XRT and shown in Figs 1-6. Listed also are their asymptotic temporal index α_X obtained from the fits and their photon spectral index Γ_X measured with the Swit X-ray telescope (XRT).

GRB	t_i [s]	$\gamma_0\theta$	t_{break} [s]	p_e	χ^2/dof	α_X ,	Γ_X
060729	310	1.723	32876	2.096	1.39	1.548	2.04 ± 0.04
061007	40	0.908	135	2.052	1.00	1.526	2.01 ± 0.10
120422A	276	1.203	84256	1.958	0.69	1.458	2.01 ± 0.25
060614				1.98	1.22	1.98	1.90 ± 0.09
110808A	100	Shotgun	17692	2.195	1.04	1.09	2.34 ± 0.22
090618	310	0.708	2953	2.083	1.06	1.54	2.00 ± 0.10

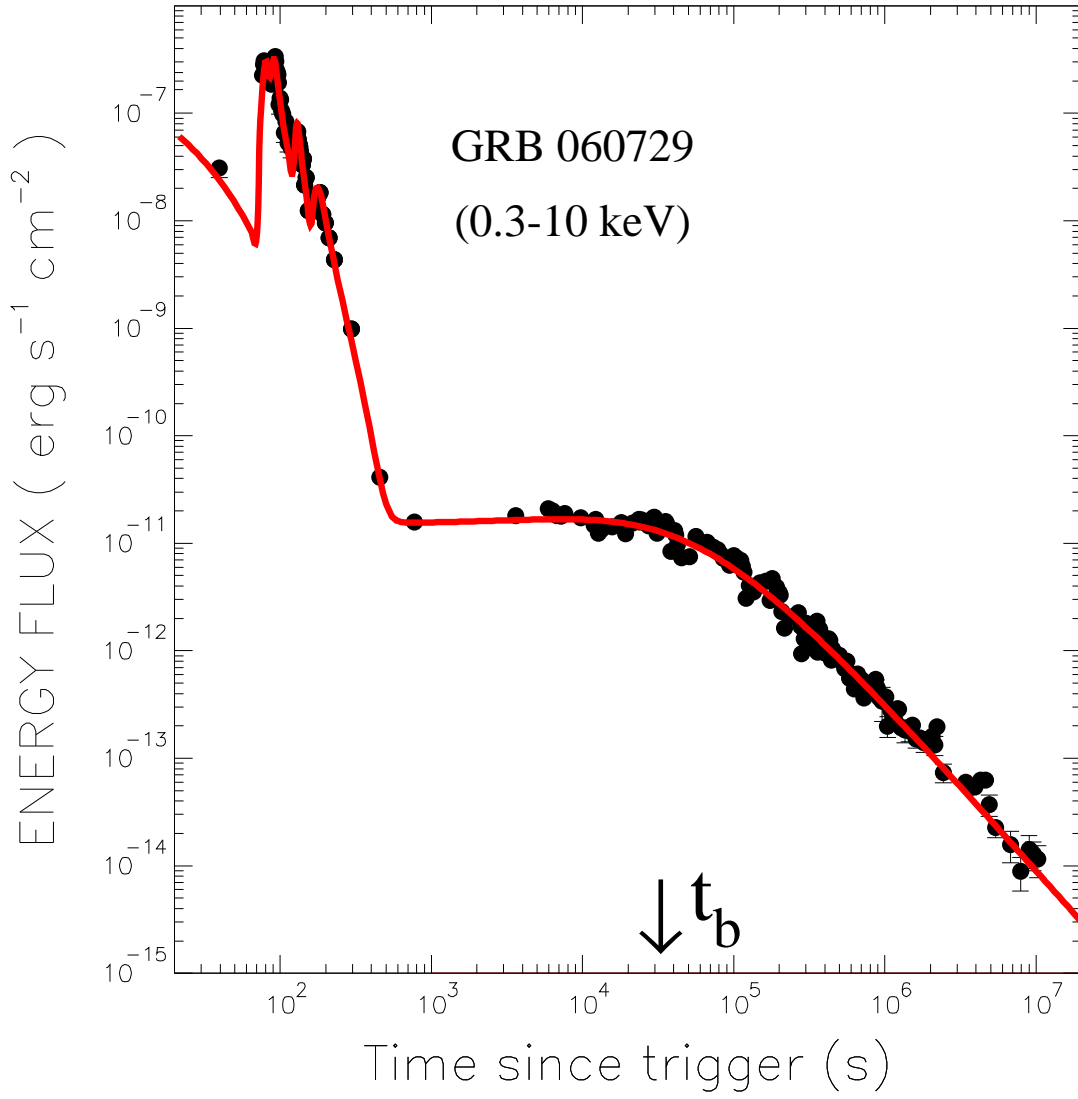


Fig. 1.— The X-ray light-curve of GRB 060729 and its CB model description (Dado et al. 2009a) assuming a constant density ISM and the late-time value $\beta_X = 1.02 \pm 0.04$ reported in the Swift/XRT light-curve repository (Evans et al. 2007,2009).

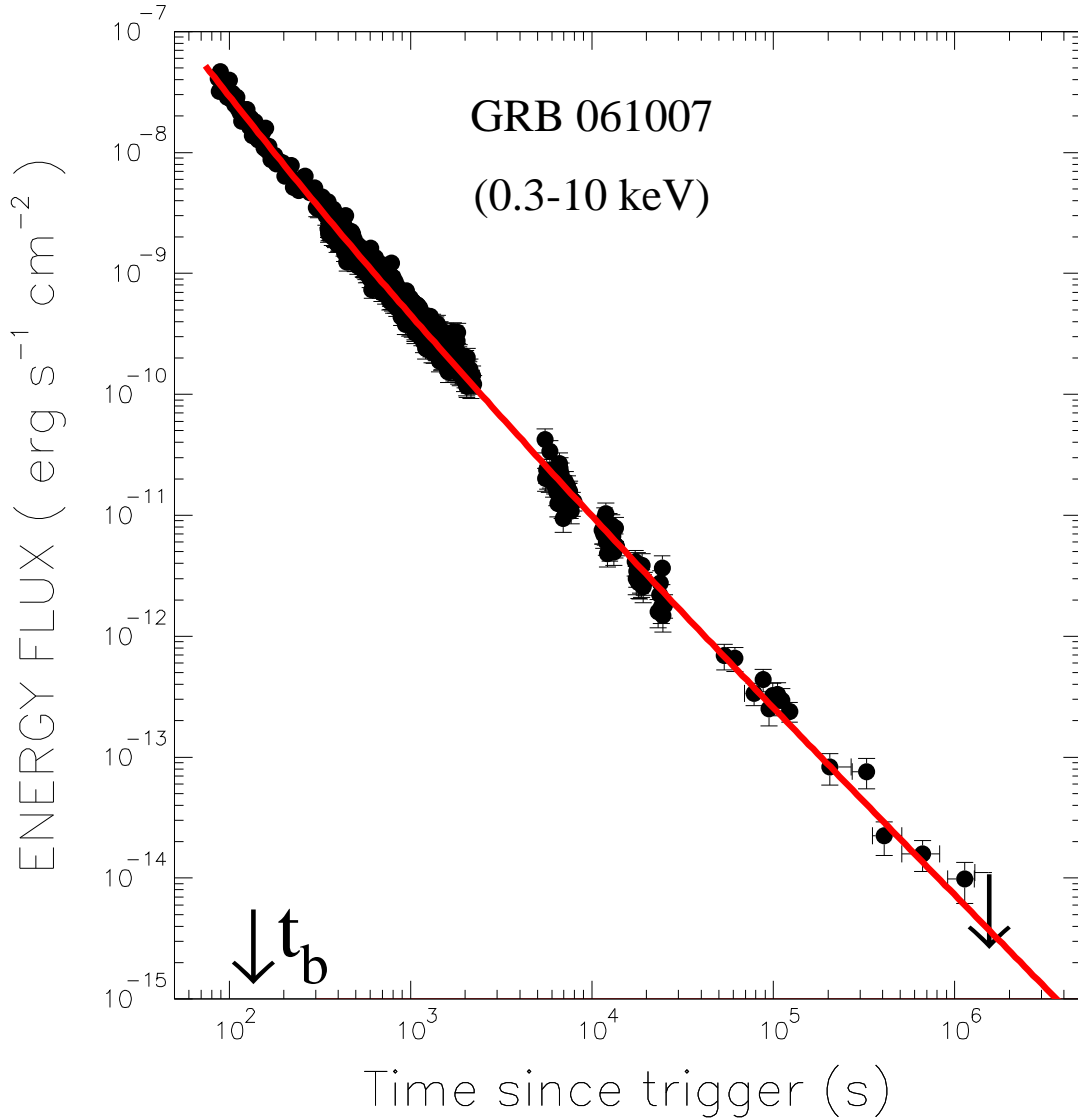


Fig. 2.— The X-ray light-curve of GRB 061007 (Evans et al. 2007, 2009) and its CB model best fit, which have yielded an early break time hidden under the prompt emission phase and a post break late-time $\alpha_X = 1.61$ (Dado et al. 2008). The photon spectral index $\Gamma_X = 2.011 \pm 0.10$ reported in the Swift/XRT light-curve repository satisfies within error the CB model relation $\alpha_X + 1/2 = \Gamma_X$.

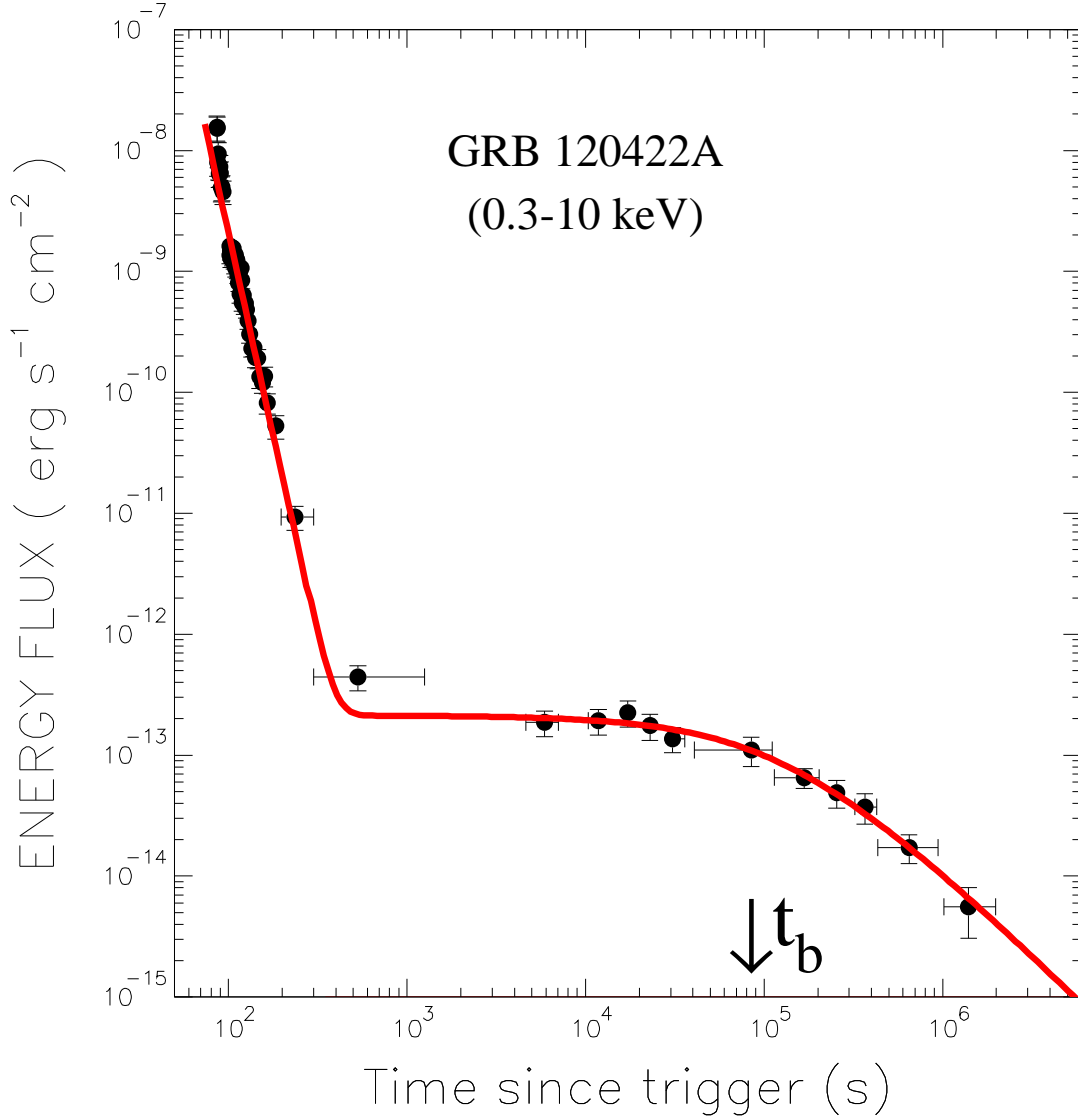


Fig. 3.— The X-ray light-curve of GRB 120422A reported in the Swift/XRT light-curve repository (Evans et al. 2007, 2009) and its CB model description assuming a constant density ISM and the best fit values $\gamma(0)\theta = 1.2$, $p_e/2 = \beta_X = 0.98 \pm 0.04$ and a break time $t_b = 84256$ s. The spectral index of the afterglow inferred from the Swift/XRT measurements in the PC mode is $\beta_X = 1.03(+0.38, -0.20)$.

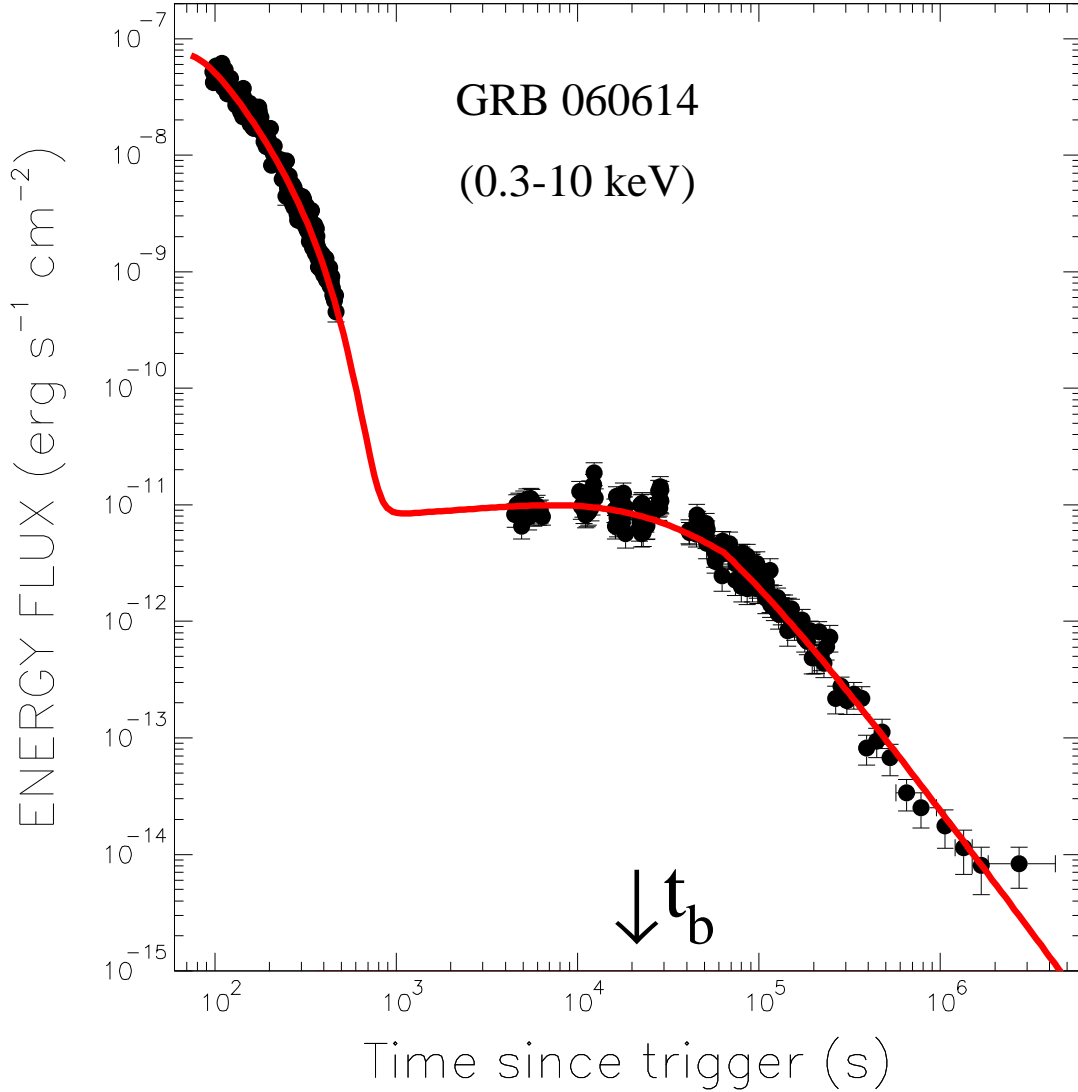


Fig. 4.— The light-curve of the 0.3-10 keV X-ray afterglow of the short hard burst 060614 and its CB model best fit (Dado et al. 2009b) assuming a late-time density profile $\propto r^{-2}$. The best fit late-time decline yields $\alpha_X = 1.98$, which implies $\beta_X = 0.98$ in agreement with the measured spectral index $\beta_X = 0.90 \pm 0.10$, which is reported in the Swift/XRT light-curve repository (Evans et al. 2007, 2009).

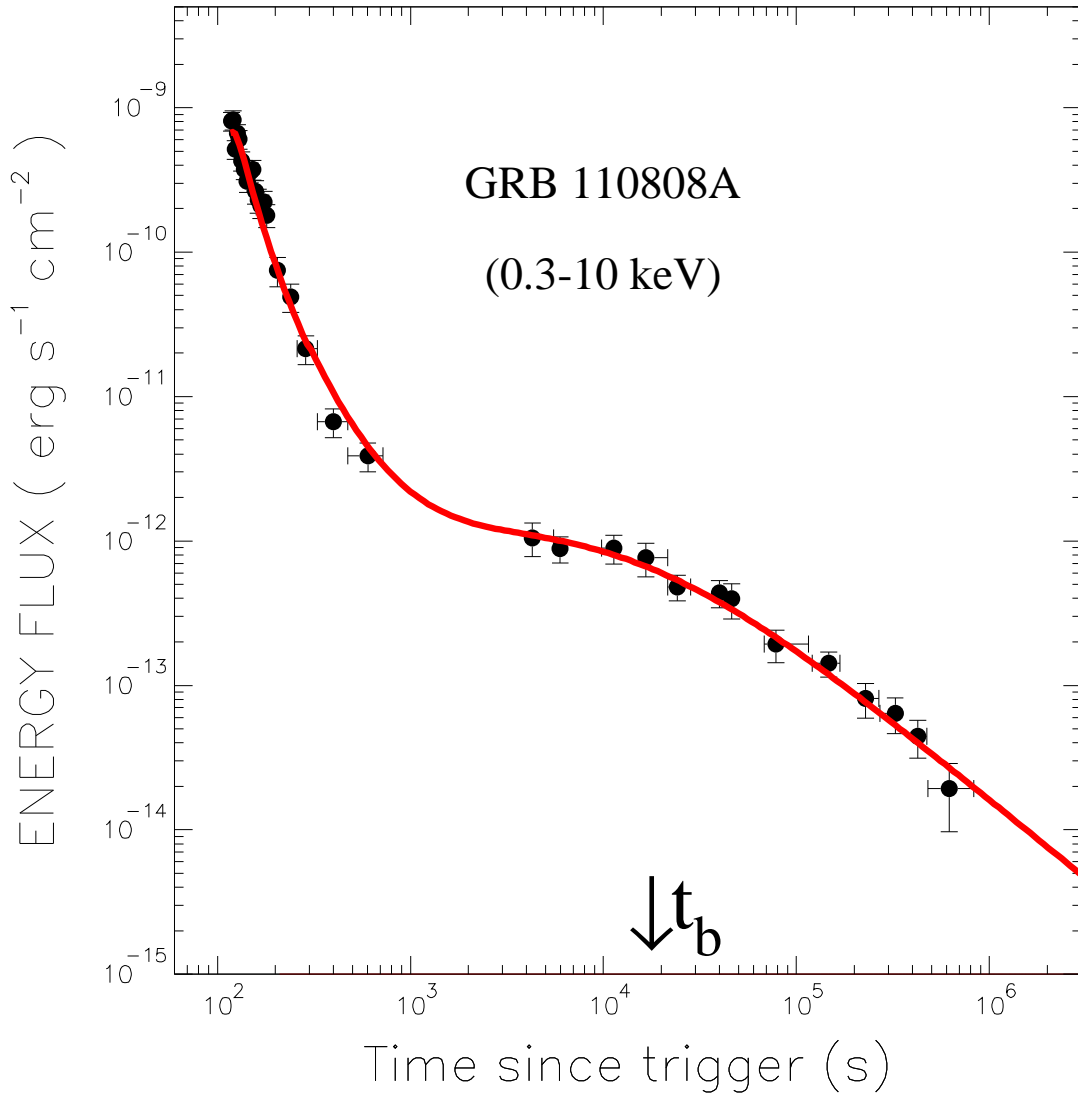


Fig. 5.— The light-curve of the 0.3-10 keV X-ray afterglow of GRB 110808A (Evans et al. 2007, 2009) and its CB model description assuming a shot gun configuration of CBs and the canonical value $\beta_X = 1.1$.

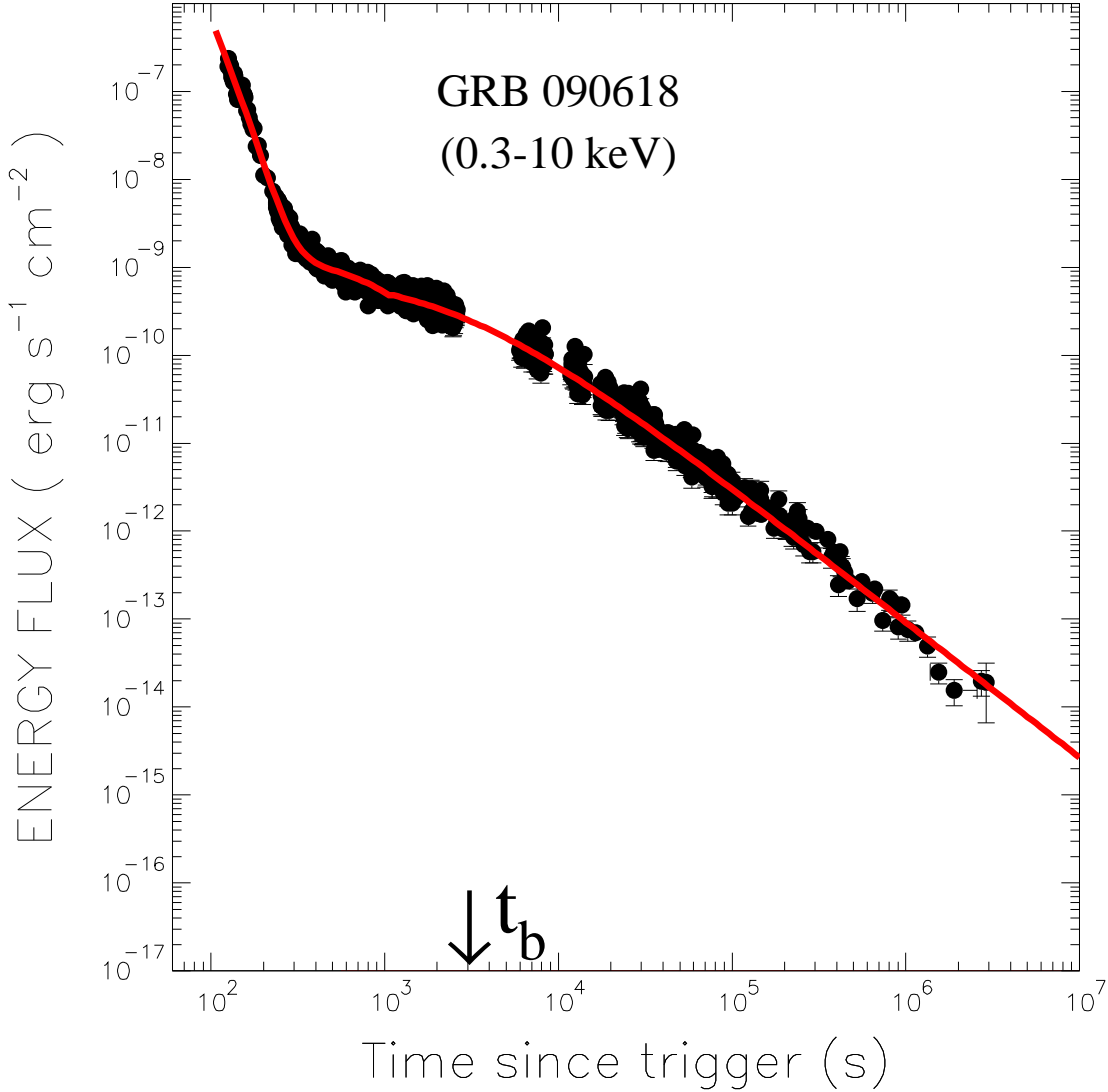


Fig. 6.— The X-ray light-curve of GRB 090618 reported in the Swift/XRT light-curves repository (Evans et al. 2007, 2009) and its CB model description assuming a constant density ISM. The best fit value $p_e = 2.08 \pm 0.09$ yields $\beta_X = p_e/2 = 1.04 \pm 0.03$, i.e., $\alpha_X = p_e/2 + 1/2 = 1.54 \pm 0.03$ and $\Gamma_X = 2.04$. The late-time spectral index inferred from the unabsorbed spectrum of the 0.3-10 keV X-ray afterglow measured with the Swift XRT (Evans et al. 2007, 2009) is $\beta_X = 1.00 \pm 0.10$ (Cano et al., 2011).

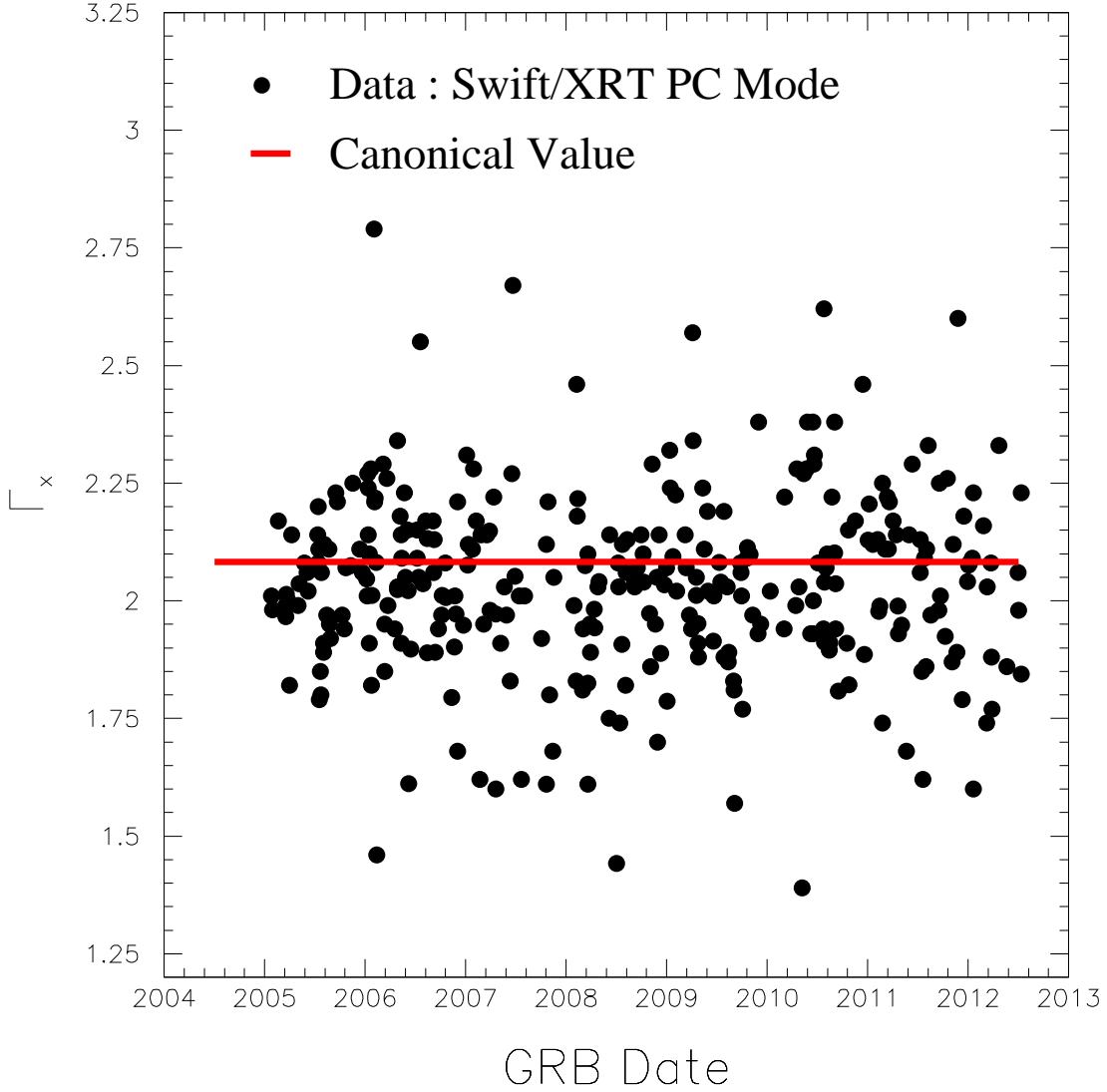


Fig. 7.— The values of the photon spectral index $\Gamma_X = \beta_X + 1$ of the 0.3-10 keV X-ray afterglow of the 315 Swift GRBs that were reported in the Swift/XRT light-curves repository (Evans et al. 2007, 2009) before August 1, 2012 whose measured light-curve extended beyond 1 day and the estimated error in their photon spectral index is < 0.25 . The horizontal line represents the CB model canonical value $\Gamma_X = 25/12 = 2.083$.

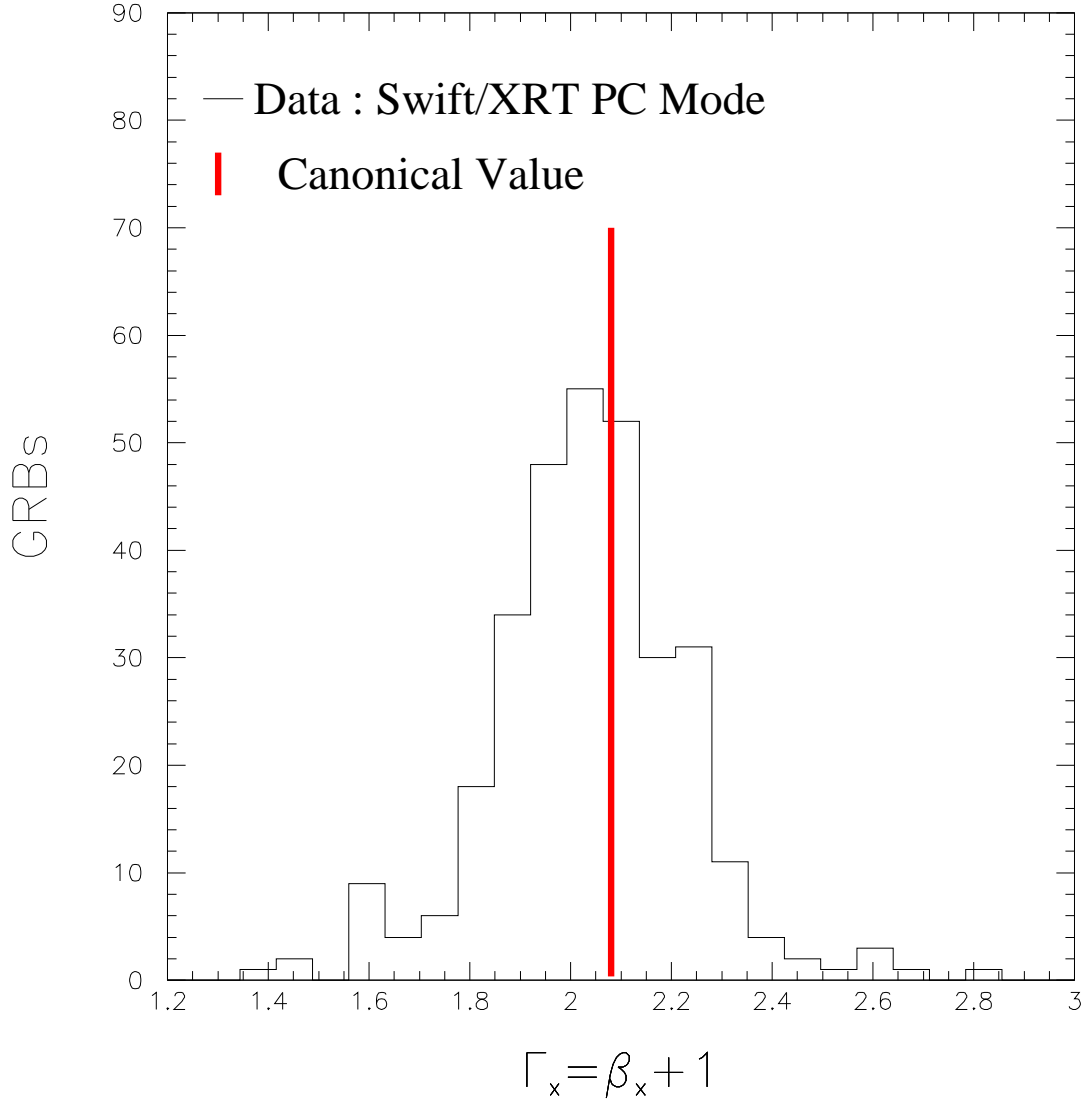


Fig. 8.— The distribution of the *late-time* photon spectral index Γ_X measured with the Swift/XRT in the PC mode for the 322 GRBs plotted in Fig. 1. The vertical line is the CB Model canonical value $\Gamma_X = 25/12 = 2.08$.

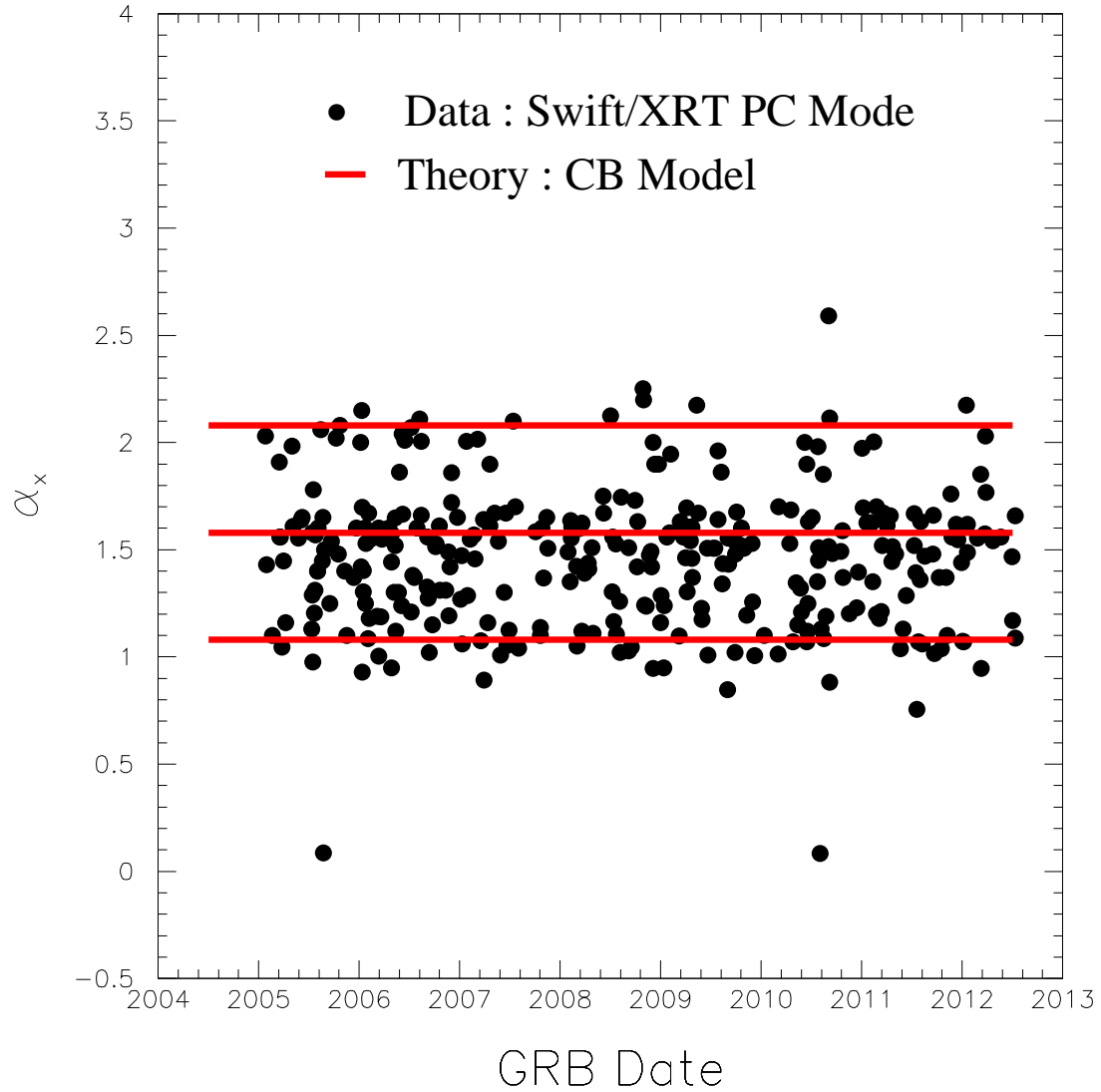


Fig. 9.— The values of the late-time temporal index α_X obtained from the CB model best fits to the the 0.3-10 keV X-ray afterglow of the 315 Swift GRBs that were plotted in Figure 7. The horizontal lines represents the CB model canonical values $\alpha_X \approx 1, 1.58$ and 2.08 .

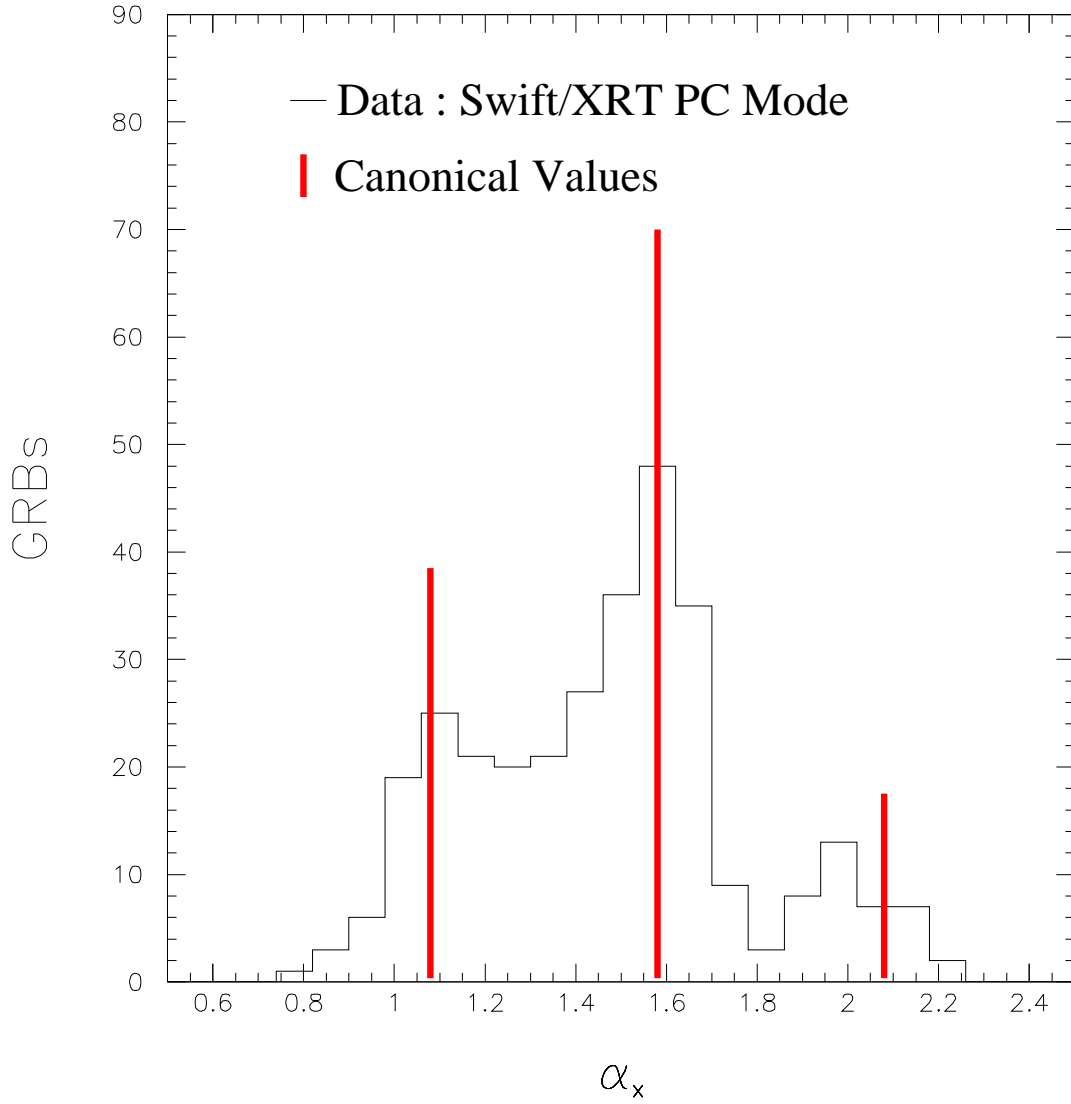


Fig. 10.— The distribution of the values of the late-time temporal index α_X obtained from the CB model best fits to the the 0.3-10 keV X-ray afterglow of the 315 Swift GRBs that were plotted in Figure 9. The vertical lines represents the CB model canonical values $\alpha_X \approx 1$, 1.58 and 2.08 .

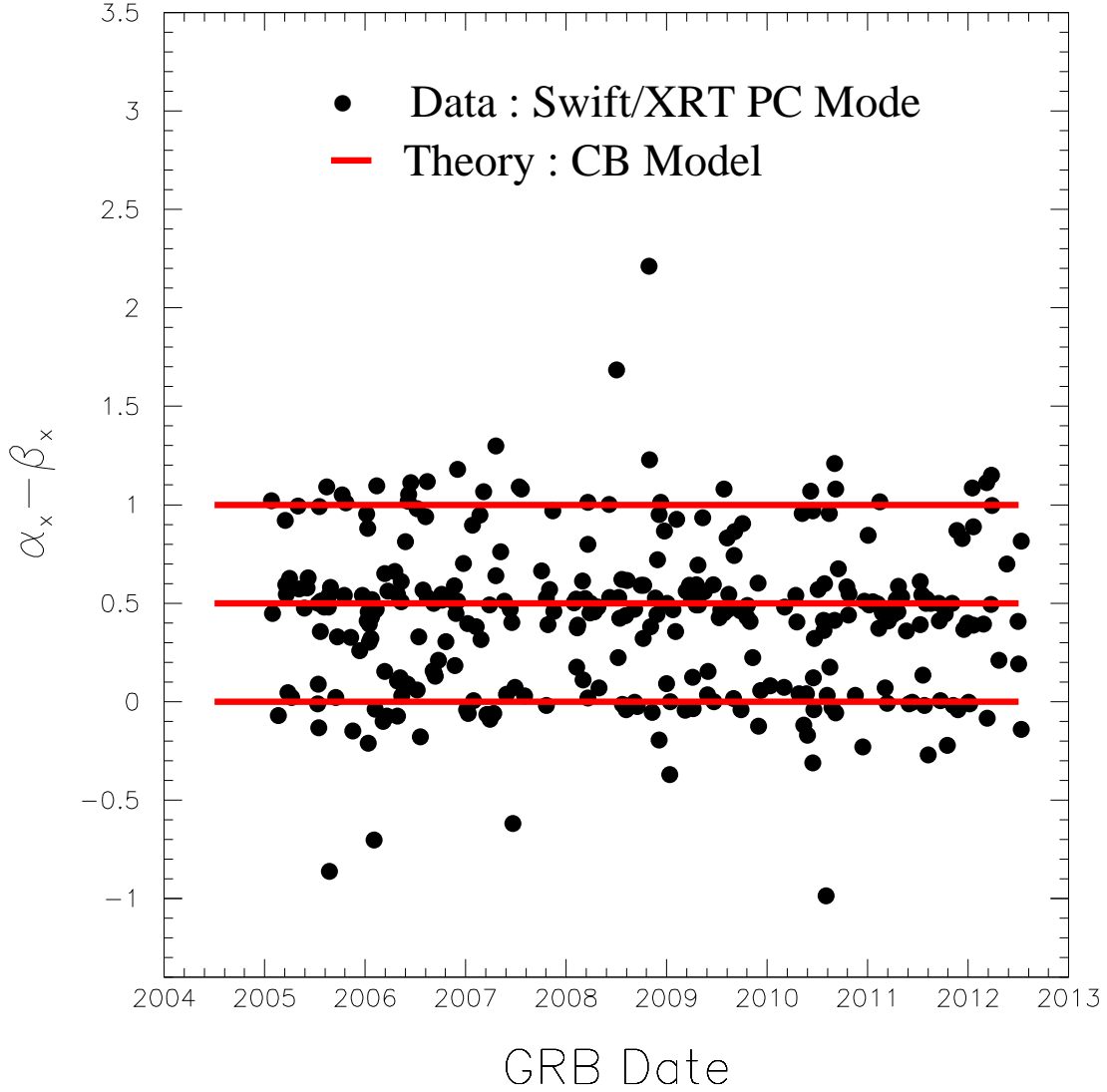


Fig. 11.— The values of $\alpha_X - \beta_X$ for the late-time 0.3-10 keV X-ray afterglow of 315 Swift GRBs detected before August 1, 2012, that are plotted in Figures 7 and 9. The horizontal lines represent the CB model expectation (see section 2) $\alpha_X - \beta_X = 0, 1/2$ or 1 for error-free measurements.

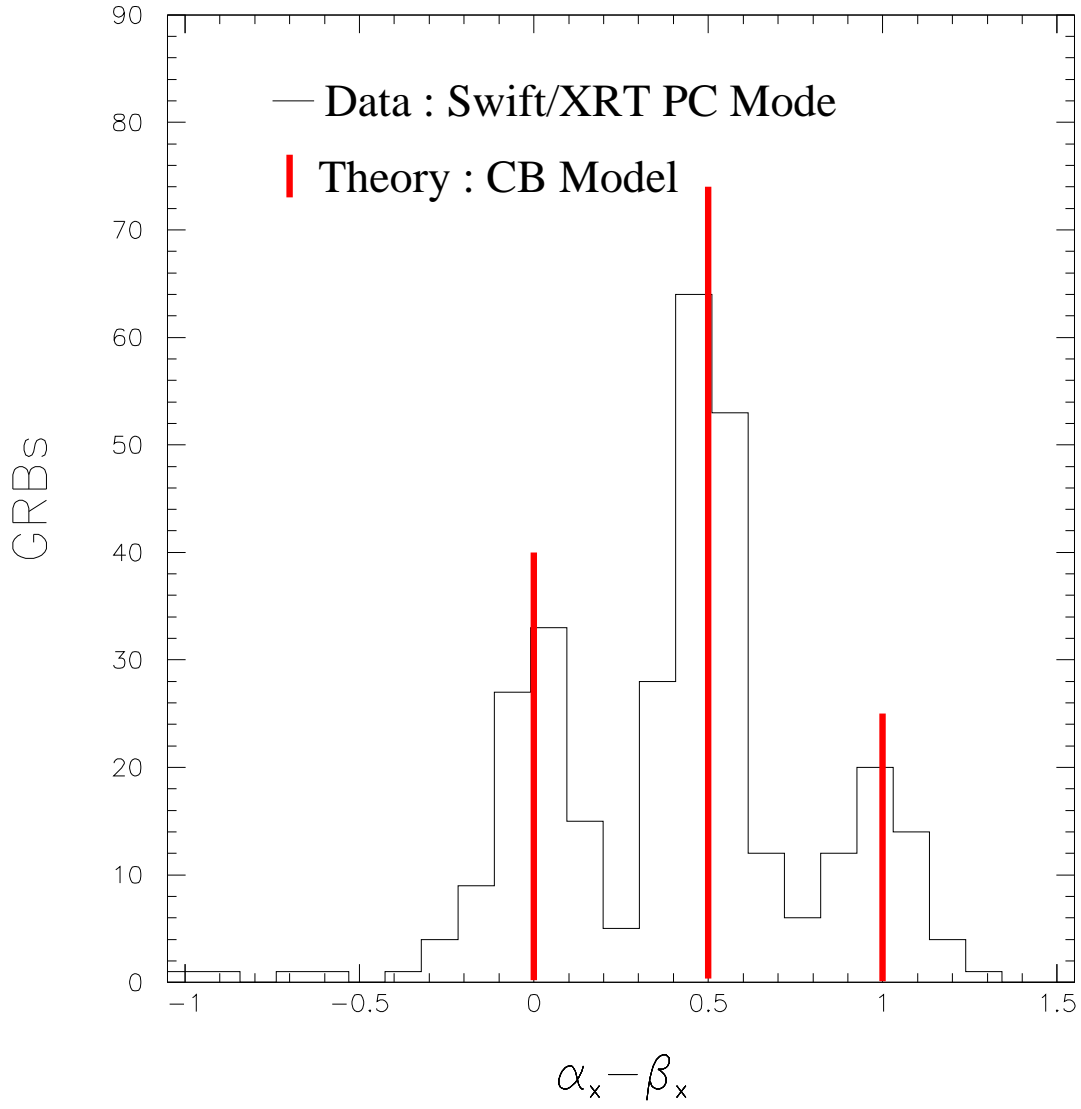


Fig. 12.— The distribution of the values of $\alpha_X - \beta_X$ which were plotted in Fig. 11 and the CB model expectation $\alpha_X - \beta_X=0, 1/2$ or 1 (vertical lines) for error free measurements.